

A functional screening platform for engineering chimeric antigen receptors with reduced on-target, off-tumour activation

Raphaël B. Di Roberto, Rocío Castellanos Rueda, Samara Frey, David Egli, Rodrigo Vazquez-Lombardi, Sai T. Reddy¹

Department of Biosystems Science and Engineering, ETH Zürich, 4058 Basel, Switzerland

¹To whom correspondence should be addressed. Tel: +41 61 387 33 68; Email: sai.reddy@ethz.ch

ABSTRACT

Chimeric antigen receptor (CAR) T cell therapies have advanced substantially in the clinic for cancer immunotherapy. However, challenges related to safety persist; one major concern is when CARs respond to antigen present on healthy cells (on-target, off-tumour response). A strategy to ameliorate this consists in engineering the affinity of CARs such that they are only activated by tumor cells expressing high antigen levels. Here, we developed a CAR T cell display platform for functional screening based on cell signaling. Starting with a CAR with high affinity towards its target antigen, we used CRISPR-Cas9 genome editing to generate a library of antigen-binding domain variants. Following multiple rounds of functional screening and deep sequencing-guided selection, CAR variants were identified that were discriminatively activated by tumor cells based on antigen expression levels. Our platform demonstrates how directed evolution based on functional screening can be used to enhance the selectivity and safety of CARs.

1 **INTRODUCTION**

2 The clinical success of chimeric antigen receptor (CAR) T cells for cancer immunotherapy has demonstrated the
3 potential of incorporating synthetic proteins in cellular therapeutics applications ¹. CARs are hybrid proteins
4 consisting of antigen-binding domains [e.g. antibody single chain variable chain fragments (scFv)] and
5 intracellular signaling domains derived from the T cell receptor (TCR): the CD3 complex and receptors mediating
6 T cell co-stimulation (e.g., CD3 ζ , CD28, 4-1BB). Following viral delivery of CAR-encoding genes into T cells,
7 the scFv enables recognition of tumour cells through surface antigen binding, while the intracellular signaling
8 domains trigger the activation of a cytotoxic response. In a clinical setting, CAR T cells with specificity against
9 the antigen CD19 have been successful in achieving partial and complete remission in patients with relapsed and
10 refractory B cell leukemias and lymphomas ^{2,3,4,5}. As with other forms of adoptive T cell therapies, CAR therapies
11 can be likened to “living drugs”, capable of achieving a sensitive, target-specific, self-amplifying and persistent
12 response. But unlike cell therapies that rely on endogenous receptors, CARs benefit from their highly modular
13 nature. For example, CAR specificity can be re-directed by engineering of the extracellular scFv domain without
14 altering the other domains, thereby enabling targeting of a wide range of malignancies. Currently, clinical trials
15 are underway to test the safety and efficacy of CARs against various tumour types and their antigens. These include
16 cancers of the pancreas, liver, breast, gut and lung, all sharing tumour-associated antigens such as HER2,
17 mesothelin, GD2 and CEA ⁶.

18

19 Although CAR therapies have shown clear clinical effectiveness against CD19-expressing B cell malignancies,
20 other cancers have proven more challenging. Several pre-clinical and clinical trials have reported instances of on-
21 target, off-tumour toxicities after CAR T administration ^{7,8,9,10}. Since healthy cells also have low-level expression
22 of tumour-associated antigens (TAAs), CAR T cells can target such healthy tissue and lead to adverse events. This
23 lack of specificity at the tissue level can be devastating for the organs affected and can require immediate treatment
24 cessation due to the risk of patient fatality ⁸. In contrast, while the CD19 antigen is also present on healthy B cells,
25 B cell aplasia resulting from CAR therapy is a manageable condition. The use of CAR T cells against non-CD19
26 cancers will thus require novel solutions in order to avoid serious adverse effects. HER2 is a prime immunotherapy
27 antigen due to its overexpression in a wide range of cancers, most notably in mammary tumours ¹¹, and its validity
28 as a therapeutic target is well supported by the long success of the monoclonal antibody trastuzumab (Herceptin)
29 in improving patient survival ¹². While a T cell-based therapy targeting HER2 has the potential to induce a long
30 term, persistent response, the downregulation of surface MHC-I in HER2-overexpressing cells makes this
31 challenging ^{13,14}. CARs constitute an attractive alternative to the TCR, as they do not rely on MHC-based antigen
32 presentation. Targeting HER2 with a CAR derived from the trastuzumab antibody was an effective strategy in a
33 xenograft study ¹⁵, but proved fatal to a patient in a subsequent clinical trial ⁸. The respiratory distress and cytokine
34 storm that followed CAR T cell injection were attributed to low levels of HER2 surface expression on normal lung
35 epithelial cells.

36

37 Various strategies have been explored for improving the cell and tissue specificity of CAR T cell therapy. One
38 common approach takes advantage of combinatorial antigen recognition, which involves the use of multiple
39 receptors ^{16, 17, 18, 19} and/or soluble targeting molecules ^{20, 21} to induce logical decision-making in CAR T cells.
40 Alternatively, the incorporation of suicide genes can be used to rapidly shut down a treatment gone awry ²².
41 However, all these approaches require the genomic integration of multiple transgenes or a combination of

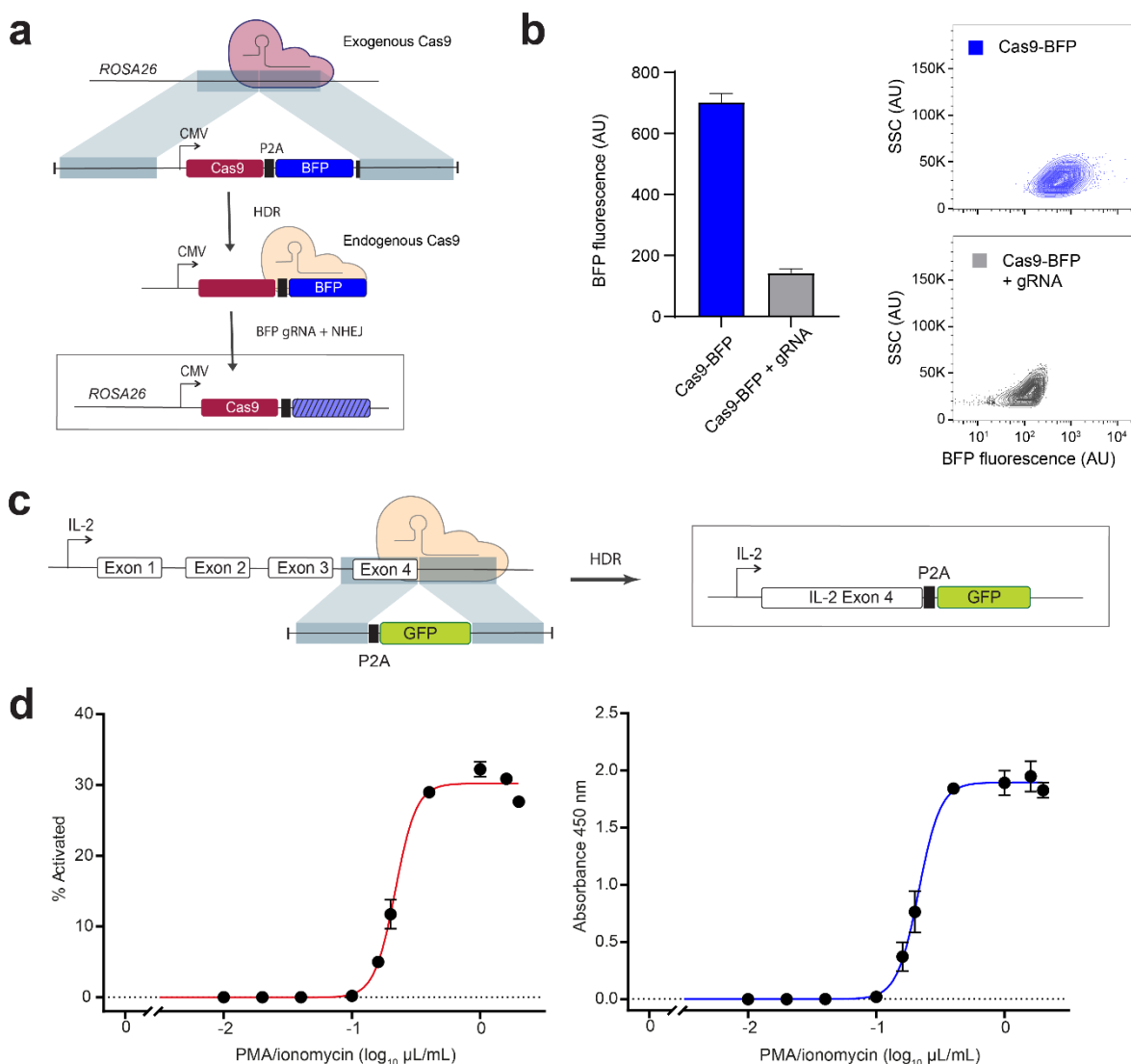
42 transgenes and biologics, making an already complex therapy even more difficult to administer. Tuning the antigen
43 binding affinity of a CAR scFv domain offers a simpler solution that is enabled by the existence of an apparent
44 maximal T cell response above a receptor affinity threshold ²³. This process typically involves selecting low
45 affinity antibody or scFv variants from random or rational libraries and “exporting” the best candidates to a CAR
46 format for further testing ^{24, 25, 26, 27, 28, 29}. However, since the threshold for selectivity is unknown and may be
47 context-dependent, many promising candidates fail once they are expressed as CARs.

48
49 Here, we report a T cell platform for CAR display that enables the engineering of variants based on antigen binding
50 and/or signaling-based screening. Development of the platform required multiple steps of CRISPR-Cas9 genome
51 editing, most notably the targeted integration of CAR genes into the unique genomic locus of the variable domain
52 of the TCR β chain. As a measure of functionality, a green fluorescence reporter (GFP) reporter gene was
53 integrated downstream of the endogenous interleukin-2 (IL-2) gene, facilitating high-throughput screening of
54 activated T cells by fluorescence-activated cell sorting (FACS). We validated this functional screening approach
55 by tuning the affinity of a CAR scFv domain with specificity towards the clinically relevant breast cancer antigen
56 HER2. Starting with a scFv derived from the HER2-targeting therapeutic antibody trastuzumab, we generated a
57 deep mutational scanning (DMS) library of CAR variants directly in our T cell platform via Cas9-mediated
58 homology-directed repair (HDR). This library was then subjected to a series of iterative selection rounds based on
59 IL-2 signaling activation following co-culture with a high-HER2-expressing cell line (SKBR3). For comparison,
60 we also selected both weak and strong binders using soluble HER2 antigen. Deep sequencing was used to identify
61 potential CAR variants that had lower binding affinity while maintaining similar signaling activation. Several
62 variants from the signaling-based selection process showed enhanced discriminative recognition of target cells in
63 a scenario mimicking on-target, off-tumour effects. These findings demonstrate the value of tuning CARs by using
64 functional signaling-based screening and could be used as a general strategy for engineering CARs with both fine
65 antigen specificity and target cell selectivity.

66
67 **RESULTS**

68 *Genome engineering of a T cell platform for CAR display and functional screening*

69 We generated a CAR display platform through a series of CRISPR-Cas9-based genome editing steps in the murine
70 T hybridoma cell line B3Z ³⁰. Previous work has shown that constitutive Cas9 expression in a cell line significantly
71 enhances efficiency of non-homologous end joining (NHEJ) and HDR ³¹. Therefore, as our first step, we targeted
72 the genomic safe-harbour locus *ROSA26* with exogenous Cas9 protein complexed with guide RNA (gRNA) and
73 an HDR template encoding genes for Cas9 and blue fluorescent protein (BFP) under the control of the human
74 CMV promoter (Figure 1a). This integration was confirmed by PCR amplification and Sanger sequencing
75 (Supplementary Figure 1a, c). The functionality of endogenous Cas9 was subsequently affirmed through the
76 NHEJ-mediated knock out of the BFP gene by transfecting BFP-targeting gRNA alone (Figure 1b).



77

78 **Figure 1: Engineering a reporter of IL-2 signaling in T cells by genome editing**

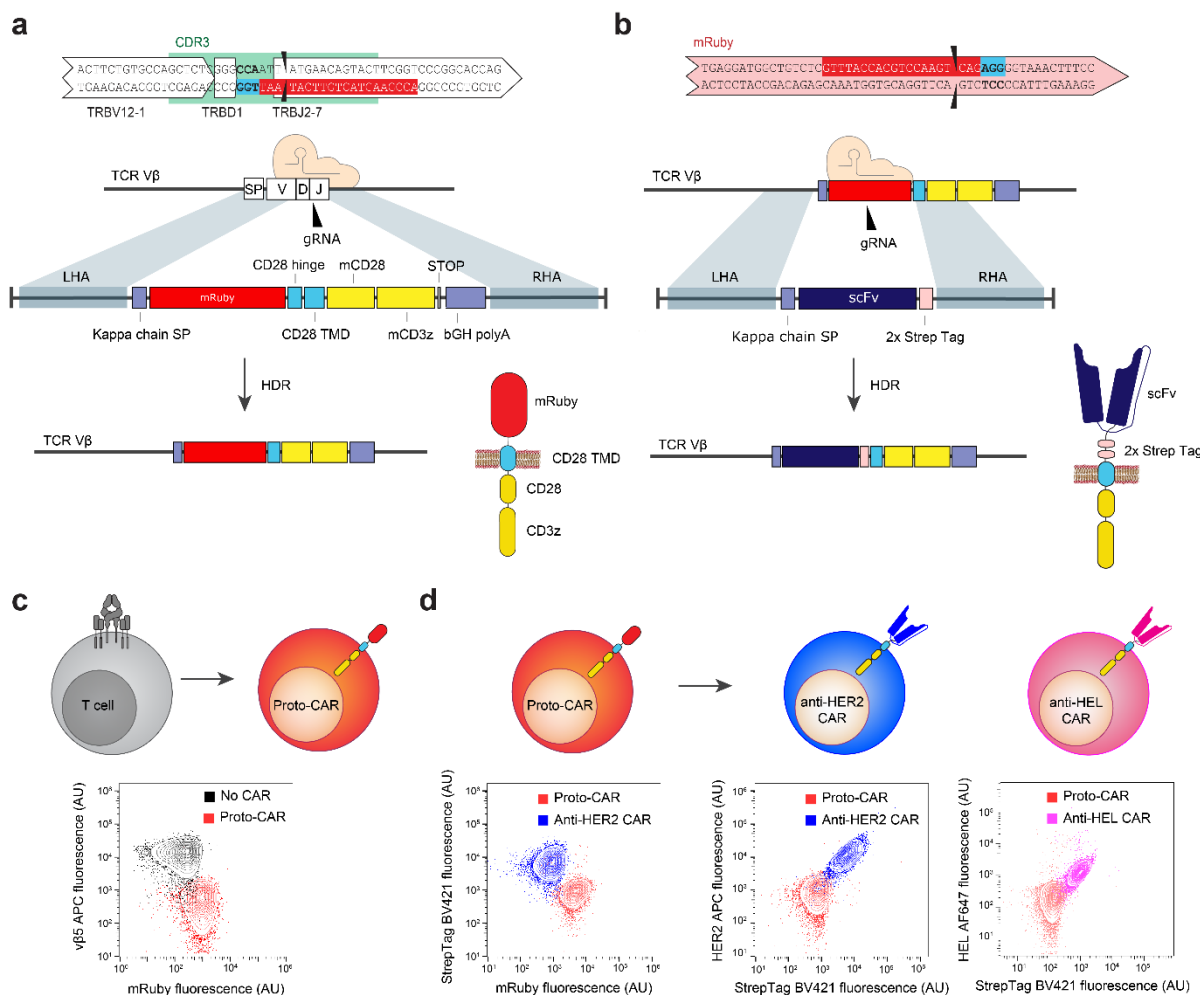
79 **a** Integration of a Cas9 expression cassette in the genome of the B3Z T cell line at the safe harbour *ROSA26* locus
80 using exogenous Cas9 protein and guide RNA (gRNA). The expression cassette consists of a gene encoding the
81 Cas9 ORF, a P2A self-cleaving peptide sequence, and a BFP ORF under the control of the human cytomegalovirus
82 (CMV) immediate-early enhancer and promoter. The constitutive expression of endogenous Cas9 was thereafter
83 confirmed by the efficient disruption of the BFP ORF through the electroporation of BFP-targeting gRNA alone.

84 **b** Histogram and flow cytometry plots showing difference in fluorescence between T cells expressing Cas9 before
85 (blue population) and after (grey population) the knockout of BFP by gRNA electroporation. **c** Integration of a
86 P2A peptide and GFP ORF immediately downstream of the final ORF of IL-2 in the genome of the Cas9-
87 expressing B3Z cell line. **d** Dose-response curve of IL2-GFP expression in engineered T cells. Following overnight
88 incubation with varying concentrations of the cell stimulation cocktail PMA/ionomycin (1X: 2 μ L/mL), cells and
89 culture supernatants were collected and assayed. The fraction of GFP-positive cells was measured by flow
90 cytometry while IL-2 levels were measured by ELISA. The fraction of activated cells (red curve) matches the IL-2
91 secretion (blue curve) in terms of sensitivity, confirming that GFP fluorescence is a suitable reporter of IL-2
92 secretion.

93

94 IL-2 cytokine secretion is a reliable marker of T cell activation following antigen engagement and co-stimulation.
95 Therefore, in order to generate a signaling reporter suitable for high-throughput screening, we used Cas9-mediated
96 HDR to integrate a GFP open reading frame immediately downstream of the last exon of the endogenous IL-2
97 gene (Figure 1c), which was once again confirmed by PCR amplification and Sanger sequencing (Supplementary

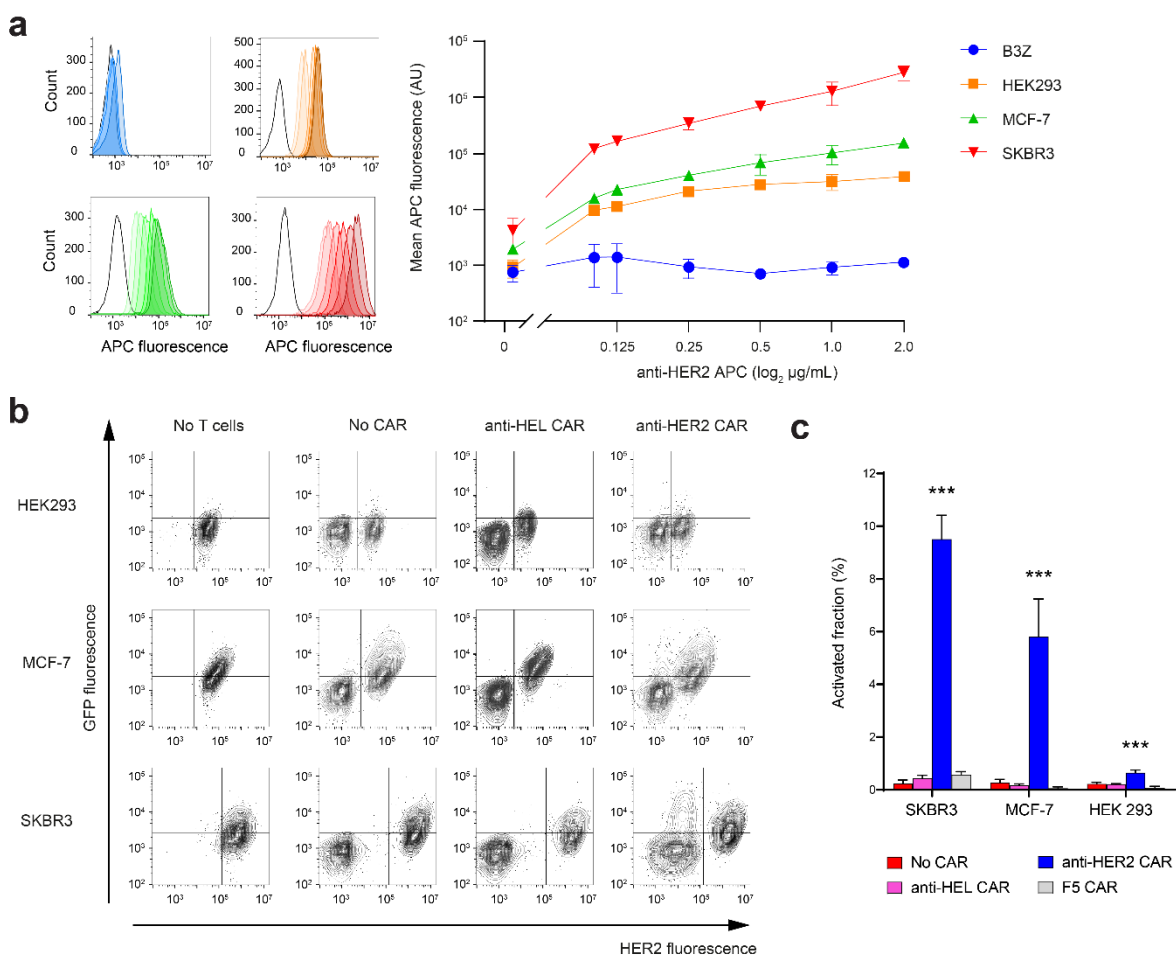
98 Figure 1b, d). An intervening P2A peptide ensures that GFP is not fused and secreted along with the cytokine. We
 99 confirmed by enzyme-linked immunoabsorbance assay (ELISA) that the genome edited T cells were still able to
 100 secrete IL-2 upon stimulation with a T cell activation cocktail of PMA/ionomycin. Interestingly, we found that the
 101 fraction of cells expressing GFP (not mean GFP intensity) scaled with cocktail concentration, and that the resulting
 102 dose-response curve matched well with that of IL-2 secretion (Figure 1d, Supplementary Figure 2). This binary
 103 response stands in contrast to previous work involving other T cell signaling reporters, such as nuclear factor of
 104 activated T cells (NFAT) ^{32, 33, 34}, and may reflect our use of the endogenous IL-2 promoter. Going forward, we
 105 used the fraction of GFP-expressing cells as our T cell activation metric.



106
 107 **Figure 2: CAR expression and antigen binding in a T cell display platform**
 108 **a** CRISPR-Cas9 HDR is used for integration of a prototypical CAR (proto-CAR) in the unique CDR β 3 region of
 109 the TCR β chain locus of engineered B3Z T cells. Double-stranded DNA with left and right homology arms (LHA
 110 and RHA) serves as repair template. A splice acceptor ensures that the CAR is on the same transcript and a signal
 111 peptide directs the protein to the secretory pathway. The proto-CAR includes a standard chassis with the CD28
 112 hinge, transmembrane domain and co-signaling domain, and the CD3 ζ signaling domain. The fluorescent protein
 113 mRuby is on the extracellular side of the CAR, as a placeholder for an scFv of choice. **b** CRISPR-Cas9 is used to
 114 replace the mRuby domain of the proto-CAR for a scFv and two Strep tags for detection. **c, d** Sequential genome
 115 engineering of T cell lines for the display of CARs with flow cytometry plots confirming CAR expression. The
 116 integration of the proto-CAR disrupts the surface expression of the endogenous TCR. This proto-CAR is then
 117 targeted to introduce an scFv of choice, such as one targeting the tumour antigen HER2 (blue cell schematic) or
 118 the model antigen HEL (pink cell schematic). The swapping of mRuby for an scFv can be detected by flow
 119 cytometry as the abrogation of mRuby fluorescence, the presence of a Strep tag II and the ability to bind labeled
 120 antigen.

121
122 Our next step was to genome engineer our reporter T cell line for CAR surface expression and signaling. The B3Z
123 cell line expresses a TCR specific for an ovalbumin-derived peptide (SIINFEKL) presented on MHC-I ³⁰.
124 Therefore, we chose to target the TCR variable β chain complementarity determining region 3 (CDRβ3) for Cas9-
125 mediated HDR of a CAR gene construct. Because of the diversity of V(D)J recombination, the CDRβ3 represents
126 a unique genomic target site, which ensures that CAR expression is limited to a single variant per cell, eliminating
127 confounding effects that can result from the multi-allelic or multi-site integration of different CAR variants.
128 Targeting CAR integration into the Vβ chain locus also simultaneously ensures knock-out of the endogenous TCR.
129 To provide a chassis for rapid CAR specificity changes, we first integrated a “proto-CAR” at the CDRβ3 locus.
130 This CAR gene chassis is composed of the hinge and transmembrane domains of CD28 and the intracellular
131 signaling domains of CD28 and CD3ζ, while lacking a typical binding domain, harbouring instead the fluorescent
132 protein mRuby on its extracellular side (Figure 2a). The expression of mRuby provides a fluorescence reporter
133 that can be used to easily detect HDR ³⁵. We first confirmed integration by PCR amplification and Sanger
134 sequencing (Supplementary Figure 1e) and then by flow cytometry we confirmed that this proto-CAR was
135 expressed and that TCR expression was abrogated (Figure 2c). Next, we electroporated cells with gRNA targeting
136 mRuby and HDR templates encoding scFv genes specific against the model antigen Hen Egg Lysozyme (HEL)
137 (variant M3 ³⁶) or human breast cancer antigen HER2 (variant 4D5/trastuzumab ³⁷) (Figure 2b). Surface expression
138 of CARs was confirmed by the presence of two Strep tags in the linker region between the scFv and the CD28
139 hinge domain. The ability of the CARs to bind their respective target antigens was also confirmed using soluble
140 fluorescently-labeled cognate antigens (Figure 2d).

141
142 *CAR T cell signaling is activated with both high and low HER2-expressing cells*
143 We next determined if our CAR T cell display platform expressing the anti-HER2 scFv could be activated
144 following co-culture with HER2-expressing cell lines. We first selected a panel of cancer cell lines known to
145 express different levels of HER2 on their surface ³⁸. Flow cytometry confirmed that SKBR3, MCF-7 and HEK293
146 cells express decreasing levels of surface HER2 (Figure 3a). These cell lines therefore provide a model system for
147 evaluating on-target, off-tumour toxicity of CAR T cells whereby SKBR3 represent tumour cells (high expression
148 of HER2) and MCF-7 and HEK293 mimic off-target healthy cells (low expression of HER2). These cell lines were
149 then co-cultured with CAR T cells expressing anti-HER scFv or anti-HEL scFv (negative control) and activation
150 was measured through IL-2-linked GFP expression via flow cytometry (Figure 3b and c). Correlating with the
151 amount of HER2 expression on the different cell lines, we observed substantial anti-HER2 CAR T cell activation
152 in the presence of SKBR3 and MCF-7 cells, but not with HEK293, while anti-HEL CARs failed to elicit significant
153 T cell activation with any co-cultured cells. We also tested a CAR based on the phage-derived scFv F5 for which
154 affinity is estimated to be 275-fold lower than 4D5 ^{26, 39} but it was shown to be largely unresponsive to our cell
155 lines. Interestingly, T cell activation appeared to correlate with trogocytosis, the transfer of antigen from target
156 cells to lymphocytes, which is consistent with a recent study ⁴⁰.



157

158 **Figure 3: A CAR with a high affinity scFv shows a limited ability to discriminate between cell lines**
159 **expressing different antigen levels**

160 **a** Surface HER2 expression levels across the cell lines used in this study. Each cell line was stained with varying
161 concentrations of anti-HER2 monoclonal antibody labeled with APC. Fluorescence was measured by flow
162 cytometry and plotted in frequency histograms as follow: top left plot: B3Z; top right plot: HEK293; bottom left
163 plot: MCF-7; bottom right plot: SKBR3. Mean fluorescence was plotted for all cell lines as a function of antibody
164 concentration. SKBR3 shows the highest surface HER2 expression, followed by MCF-7, HEK293 and B3Z in
165 descending order. **b** CAR T cells possessing a high affinity anti-HER2 scFv domain (4D5) were co-cultured with
166 HER2-expressing cell lines. Following a 16-hour co-culture, cells were collected and flow cytometry was
167 performed to measure HER2 and GFP expression. **c** Percentage of GFP-expressing T cells after co-culture with
168 HER2-expressing cell lines. T cells expressing the Herceptin-derived anti-HER2 CAR showed a significant
169 response to each tumour cell line compared to no CAR. Mean and S.E.M. were obtained from two independent
170 experiments conducted with triplicates. For assessing significance, Dunnett's multiple comparisons test was used
171 with the following indicators: * $P < 0.01$, ** $P < 0.001$, *** $P < 0.0001$.

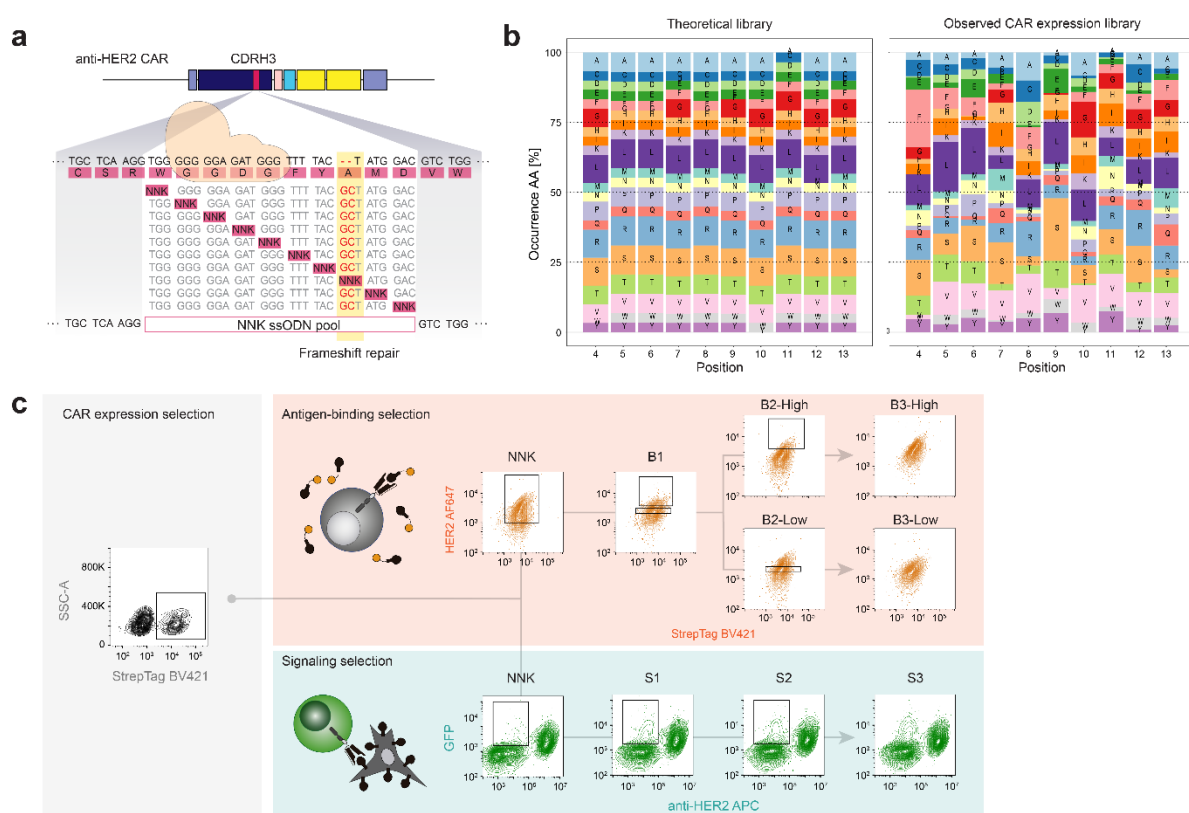
172

173 *Mutagenesis of a CAR and screening by antigen-mediated signaling or binding*

174 The significant T cell activation encountered in the presence of both SKBR3 and MCF-7 cells suggested that the
175 anti-HER2 CAR was not able to discriminate effectively between the antigen levels of each cell line. This is likely
176 due to the very high affinity of the 4D5 scFv clone (equilibrium dissociation constant, $K_d \sim 0.1 \text{ nM}$ ²⁶). Using
177 SKBR3 and MCF-7 cells to model tumour and healthy cells, respectively, we thus proceeded to use our T cell
178 platform to engineer CAR variants that would retain activation in the presence of SKBR3 cells but show a reduced
179 signalling response to MCF-7 cells. Our engineering strategy was based on the possibility of tuning the binding
180 affinity of the scFv domain, such that a higher density of antigen molecules on the target cell's surface is needed

181 for successful T cell activation, thereby enabling greater cell-level selectivity. We hypothesized that our platform
 182 was suitable for this application as introducing mutations in the scFv domain will generate variants with different
 183 binding affinities and the IL-2-based signaling reporter could then be used to select for variants retaining
 184 responsiveness to HER2 on SKBR3 cells.

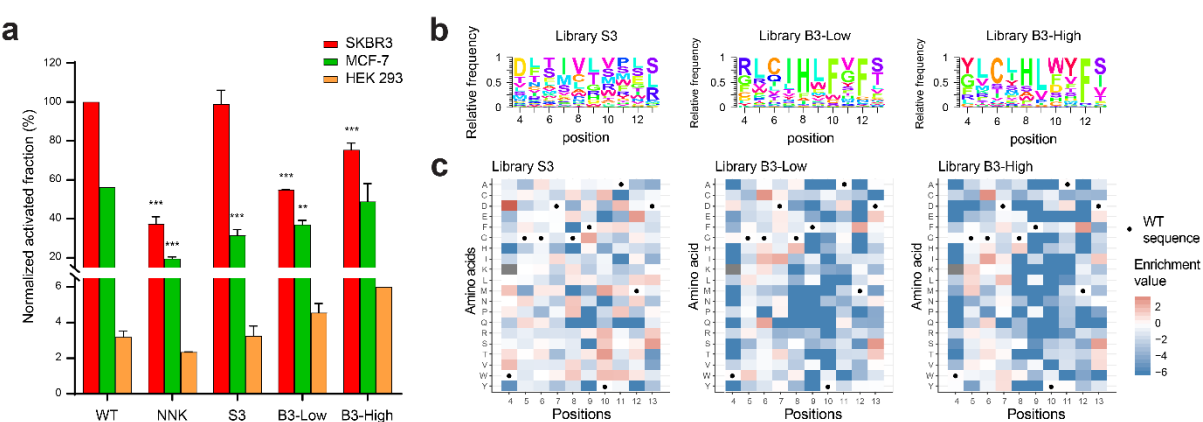
185
 186 In order to generate a library of CAR variants with diverse HER2 antigen binding affinities, we performed deep
 187 mutational scanning (DMS) on the scFv domain. Specifically, we focused on the complementarity-determining
 188 region 3 of the variable heavy chain (CDRH3), which is a major determinant of binding specificity⁴¹. The library
 189 was generated directly in T cells by genome editing, where Cas9 is used to integrate a pool of single-stranded
 190 oligodeoxynucleotide (ssODN) HDR templates to a pre-existing construct^{31, 42}. The HDR templates were based
 191 on a DMS design of a single-site saturation mutagenesis library, where degenerate codons (NNK; N = A, C, G, T;
 192 K = G, T) are tiled across the 10 amino acids of the CDRH3 (Figure 4a). DMS libraries were screened and selected
 193 by FACS for cells with CAR surface expression based on Strep tag display. Next, deep sequencing was performed
 194 to assess the sequence landscape associated with CAR surface expression, demonstrating the expected diversity,
 195 with 190 out of possible 191 variants present and no apparent selection bias (Figure 4b).
 196



197
 198 **Figure 4: Generating a deep mutational scanning (DMS) library of CARs and selecting functional variants**
 199 **a** DMS of the CDRH3 region of the variable heavy chain of the CAR possessing the high affinity anti-HER2 scFv
 200 domain (4D5). The original anti-HER2 CAR was disrupted by the introduction of a frameshift-inducing deletion
 201 in the CDRH3. A set of degenerate ssODNs was then used to repair this deletion by CRISPR/Cas9 genome editing,
 202 while also substituting each position with all possible amino acids in a non-combinatorial fashion, for a total of
 203 191 variants. Successful genome editing resulted in recovery of CAR surface expression, whenever possible. **b**
 204 Comparison of the theoretical (left) and observed (right) amino acid frequencies in the DMS library. Genomic
 205 DNA was extracted and the CDRH3 locus amplified and sequenced to measure the amino acid frequencies. The
 206 original 4D5 CDRH3 amino acids were not included in the histograms due to their overrepresentation. **c** FACS-

207 based selection of CAR variants according to their antigen response or binding ability. Following transfection of
208 the ssODN library, T cells expressing a CAR on their surface were selected based on Strep tag II staining (library
209 “NNK”). This library was then used in two selection strategies in parallel. In one strategy based on antigen binding
210 (“B”), a non-saturating concentration of soluble HER2 was used to select stronger (“High”) and weaker (“Low”)
211 binders iteratively. In the second strategy based on signaling (“S”), co-culture with the high HER2-expressing cell
212 line SKBR3 was followed by sorting according to GFP expression iteratively.
213

214 Next, we tested two approaches to select variants from the DMS library of CAR variants (Figure 4c). In one branch,
215 selection was performed on the basis of binding to soluble HER2 antigen (“B” libraries). Iterative rounds of sorting
216 were performed to select strong binders (B1, B2 High, B3 High) and weak binders (B1, B2 Low, B3 Low). In a
217 second branch, CAR library variants were co-cultured with SKBR3 cells and IL-2 linked GFP expression was used
218 to sort signaling responders (“S” libraries) in an iterative fashion (S1, S2, S3). The final libraries (B3-High, B3-
219 Low and S3) were compared by their ability to respond to co-cultures with each of the HER2-expressing cell lines
220 (Figure 5a and Supplementary Figure 3). The S3 library showed the highest ability to discriminate between the
221 cell lines, largely due to unchanged signaling with SKBR3 and reduced signaling to MCF-7. Conversely, the B3
222 libraries showed reduced signaling to both cell lines compared to the initial CAR. These differences could not be
223 accounted for by differences in CAR expression levels across libraries (Supplementary Figure 4).



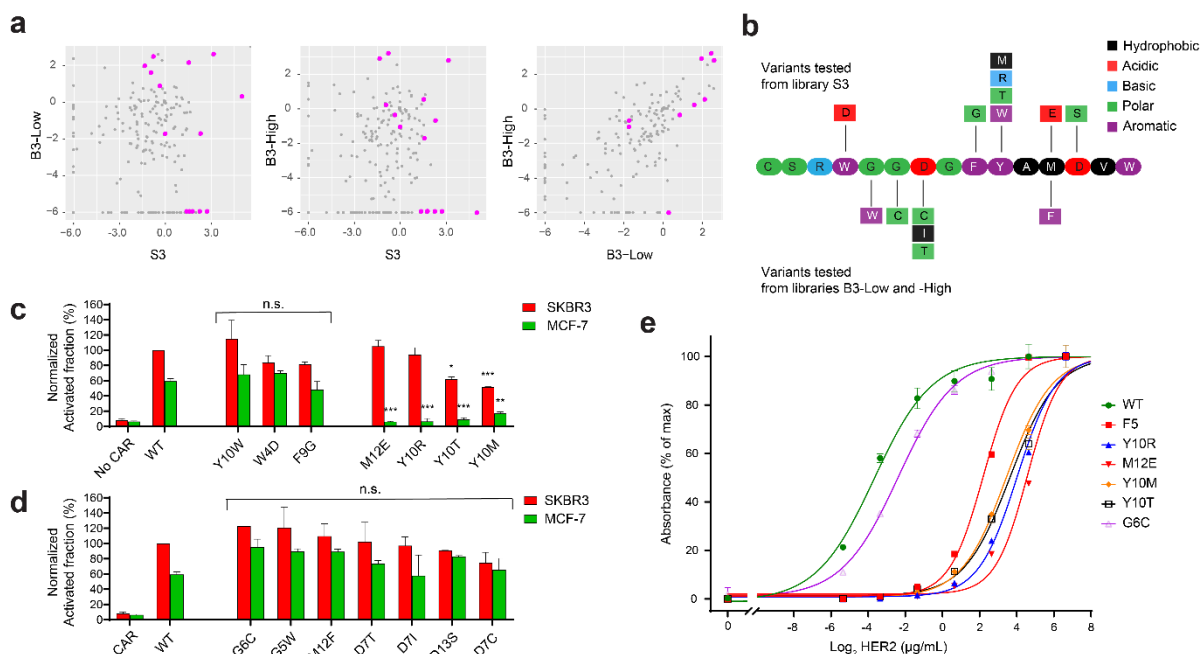
227 **a** Histogram of the response profiles of the wild-type anti-HER2 CAR T cells (WT), the initial (NNK) and the
228 endpoint (S3, B3-Low, B3-High). The T cells were co-cultured overnight with HER2-expressing cell lines and the
229 expression of GFP was measured by flow cytometry, revealing differences in the ability of libraries to discriminate
230 between antigen levels compared to WT. Mean and S.E.M. were obtained from two independent experiments
231 conducted with triplicates. For assessing significance, Dunnett’s multiple comparisons test was used with the
232 following indicators: * $P < 0.01$, ** $P < 0.001$, *** $P < 0.0001$ **b** Sequence logo plots of the relative frequencies
233 of the amino acid substitutions in the endpoint libraries. WT amino acids at each position are not shown. **c**
234 Enrichment ratios for each CAR variant in the three endpoint libraries S3, B3-Low and B3-High in heat map form.
235 Enrichment ratios were calculated as the ratio of the relative abundance of a sequence within an endpoint library
236 over its relative abundance in the initial NNK library.
237

238 *Identification of CAR variants that are selectively activated based on tumour antigen surface expression*

239 In order to identify single CAR variants showing an ability to discriminate across HER2 surface expression levels,
240 we performed deep sequencing on the final binding and signaling libraries and compared the relative frequencies
241 (Figure 5b) and the enrichment of single variants relative to the initial library (Figure 5c). The resulting enrichment
242 heatmaps revealed more negative selection (in the form of lower enrichment scores) in libraries B3-High and B3-
243 Low than for the S3 library, particularly at positions 8-12 of the CDRH3. Conversely, the S3 signaling library was

244 less constrained across the entire region and deviated strongly from the other two, suggesting that there is a
245 discordance between CAR antigen binding and signaling.

246
247 By using the deep sequencing data, we selected a set of variants from the S3 library based on high enrichment
248 (Figure 6a and b). Additionally, we selected four variants from B3-Low showing more enrichment than in B3-
249 High and three variants from B3-High. Cell lines of these CAR variants were then generated by Cas9-mediated
250 HDR and subsequently co-cultured with either SKBR3 or MCF-7 and monitored for signaling activation by IL-2
251 linked GFP expression (Figure 6c and d, Supplementary Figure 5 and 6). Among them, four variants from the S3
252 library showed significant discrimination between the high-HER2 SKBR3 and low-HER2 MCF-7 cells when
253 compared to the original CAR. Importantly, for variants M12E and Y10R, there was no reduction in responsiveness
254 towards SKBR3. None of the variants from the binding libraries were able to discriminate based on HER2 surface
255 expression, as they showed similar activation with both SKBR3 and MCF-7 cells, highlighting the difficulty of
256 using antigen-binding as the only selection approach.



257
258 **Figure 6: CAR variants enriched by signaling-based selection exhibit discriminative activated based on**
259 **HER2 cell surface expression.**

260 **a** Scatter plot of the enrichment ratios for each variant across pairs of libraries. Variants selected for further study
261 are highlighted in pink. The S3 library stands out as exhibiting little correlation to the two binding selection-based
262 libraries. **b** Schematic of the CDRH3 region and the single-substitution variants individually selected based on
263 their enrichment ratios. **c, d** Bar graphs of normalized activation (fraction of IL-2-linked GFP-positive cells) from
264 CAR variants (selected in **a**) following co-culture with either SKBR3 (high HER2 expression) or MCF-7 (low
265 HER2 expression). Four variants, selected based on signaling, (M12E, Y10R, Y10T and Y10M) respond
266 significantly less to MCF-7 and of these, two (M12E and Y10R) show no significantly reduced signaling to SKBR3
267 compared to the wild-type (WT). No variants selected based on binding show a significant difference to the WT.
268 Mean and S.E.M. were obtained from two independent experiments conducted with triplicates. For assessing
269 significance, Dunnett's multiple comparisons test was used with the following indicators: * P < 0.01, ** P < 0.001,
270 *** P < 0.0001. **e** ELISA data of antigen-binding from CAR variants expressed in soluble scFv form. The variable
271 heavy and light chains of the CAR variants were expressed in bacteria with a His tag. Following immobilization
272 on a plate with a monoclonal anti-His tag antibody, binding to varying concentrations of biotinylated HER2 was
273 detected with the addition of Streptavidin-HRP.

275 Finally, we aimed to quantitatively understand the impact of antigen-binding of our CAR variants that showed
276 discriminative activation based on HER2 surface expression. We expressed the binding domain of the CARs in
277 soluble scFv form and measured their binding to HER2 antigen by ELISA (Figure 6e). This assay revealed strong
278 decreases in binding for all of the discriminating variants. By comparison, the variant G6C, obtained by binding
279 selection, showed only a modest reduction in binding relative to the initial 4D5 scFv. Furthermore, we found that
280 the variant F5, which was largely unresponsive to SKBR3 (Figure 3c), displayed a binding curve similar to that of
281 the discriminating variants, highlighting a divergence between cell responsiveness and antigen-binding. Taken
282 together, this suggests that signaling-based selection is a superior strategy to binding-based selection for
283 identifying CAR T cell variants that can discriminate based on tumour antigen surface expression.

284

285 **DISCUSSION**

286 Through a series of genome editing steps, we have engineered a CAR T cell display platform for screening based
287 on signaling based-activation or antigen binding. We have demonstrated its value for affinity tuning, a simple and
288 yet effective method to reduce the likelihood of on-target, off-tumour effects. This approach relies on general
289 principles of genome editing and directed evolution, and has the potential to eliminate instances of toxicity early
290 in the development pipeline of CAR-based immunotherapies. The benefits of decoupling receptor affinity and T
291 cell activation were first shown by Chmielewski *et al.*, which in a study found that CARs with K_d affinity values
292 above 10^{-8} M responded strongly to high HER2-expressing cell lines in vitro, but were not activated in the presence
293 of low HER2-expressing lines, unlike their higher affinity counterparts⁴³. This result encapsulates a paradox of
294 affinity in the context of cell-mediated cytotoxicity: while high affinity theoretically implies exquisite specificity
295 at the epitope level, specificity at the cell/tissue level can in fact be impaired due to an inability to discriminate
296 between antigen levels. Furthermore, there may be additional benefits to reducing CAR affinity, such as greater
297 cell expansion and longer persistence⁴⁴. These observations are likely a factor for the characteristic low binding
298 affinity of endogenous TCRs relative to that of B cell receptors and antibodies⁴⁵. In T cell maturation, central
299 tolerance mechanisms ensure that high-affinity self-reactive T cells are removed from the immune repertoire. For
300 CAR engineering, a process must be devised with an equivalent outcome to avoid targeting cells expressing normal
301 levels of oncogenes.

302

303 Our CAR display platform closes existing gaps in current methods of tuning target selectivity. Previous examples
304 have relied on utilizing low affinity antibodies to rationally design CARs with safer target selectivity^{24, 25, 26, 27, 28,}
305 ²⁹. While our platform can also be used to rapidly assess the functionality of rationally designed variants, its true
306 strength lies in its ability to accommodate library generation and functional screening. Given the uncertainty
307 surrounding the threshold of affinity required for CAR triggering, optimizing CAR safety benefits greatly from a
308 readout for cell signaling. Here, the IL2-GFP reporter acted as a “guardrail”, preventing selected variants from
309 “falling” into non-functionality. This is especially important since the activation threshold varies across antigens
310 and epitopes^{26, 43}, and may vary across CAR signaling components (e.g., CD28 vs. 4-1BB co-signaling domain)
311 ⁴⁶. Differences in epitopes may in fact explain why no activity was observed with the CAR scFv variant F5, which
312 was derived from a phage display library screened for triggering the intracellular uptake of bound HER2³⁹. Epitope
313 mapping suggests that it targets the membrane-distal domain 1 of HER2, while the 4D5 antibody targets the
314 membrane-proximal domain 4^{39, 47}. It is not immediately clear why this difference affects CAR triggering, despite
315 the relative binding of F5 being seemingly comparable to that of our variants which maintain signaling. Until such

316 questions are resolved, a display platform such as ours that enables the detection of signaling activation ensures
317 that no prior knowledge regarding the strength of the affinity or the targeted epitope is required for optimizing a
318 CAR.

319
320 Engineering a CAR for selectivity based on tumour antigen surface expression relies on the important notion that
321 antigen-binding affinity and antigen-induced signaling strength can diverge. This is most apparent for CARs with
322 high binding affinities, where a “ceiling” is encountered above which activation does not improve further^{23, 43}.
323 This ceiling implies that reducing CAR affinity does not necessarily lead to a decline in responsiveness to a target
324 tumour, and so signaling is a more “relaxed” constraint than binding. This was evident as we attempted to also
325 select low affinity variants by antigen binding selection, but this was not successful on its own in identifying
326 variants that could discriminate on the basis of tumour antigen surface expression. A possible reason for this is
327 that our selection (gating) strategy was too conservative and did not sufficiently deviate from the B3-High strategy.
328 The difficulty of selecting an appropriate gating strategy further supports the use of signaling-based selection
329 which was trivial by contrast, merely requiring that all GFP-positive clones be selected. Furthermore, although our
330 end goal was to improve discrimination between two cell lines, SKBR3 and MCF-7, it is notable that the latter
331 played no part in our selection strategies. As the difference in antigen levels between the two cell lines was
332 relatively large, no negative selection step was required. The binding libraries might have benefited from negative
333 selection, but this was constrained by the low sensitivity of fluorescence-based binding detection, which made it
334 difficult to distinguish weak-binders from non-binders. This became especially apparent once we had obtained
335 discriminating variants by signaling selection, as these showed no detectable binding to soluble antigen by flow
336 cytometry, despite co-culture and ELISA assays confirming their function. Signaling pathways can amplify signals
337 that are mistakenly deemed too weak to trigger a response, even when the reporter includes significant signal
338 dampening through negative regulation⁴⁸. The endogenous IL-2 promoter offers a suitable sensitivity as a reporter
339 of CAR T cell activation for screening purposes.

340
341 Our affinity tuning approach also benefited from the combination of DMS, which can cover a large sequence space
342 in an unbiased way, and from deep sequencing, which revealed the substitutions that became enriched as a result
343 of different selection approaches. Performing a single-site saturation mutagenesis scan can avoid shifting the target
344 epitope too far from what has been deemed a good target site, saving us from “reinventing the wheel” by screening
345 novel variable heavy and light chain combinations. As the majority of random mutations do not improve a protein’s
346 function, we hypothesized that a combination of random mutagenesis and relaxed selection constraint would
347 broaden and left-skew the distribution of binding affinities. After a single-mutation scan, our experiment resulted
348 in a moderate improvement in antigen-level discrimination across the whole library level solely through the
349 signaling-based selection strategy, validating this approach. However, the binding selection strategies also proved
350 essential for identifying the specific mutations responsible for this phenotype. The enrichment of our best variants,
351 M12E and Y10R, did not lead them to dominate the S3 library, since the strong HER2 binding variants were not
352 depleted by the relaxed signaling-based constraints. Rather, the depletion of M12E and Y10R in the B3 libraries
353 was key for highlighting their tuned affinity. In fact, the Y10 position showed strong negative selection in these
354 libraries, revealing its value for discriminative activation. The use of DMS and parallel selection strategies thus
355 appears to be a promising method for gaining insight on key residues that can be altered without abrogating the
356 antigen-specific signaling response.

357

358 As the CAR immunotherapy field shifts towards addressing solid tumours, an increasingly diverse array of
359 antigens requires targeting, and so more instances of off-tumour toxicity will be encountered. This does not have
360 to lead to the exclusion of valid targets and abandoning the wide range of high-affinity antibodies that have been
361 discovered to date. Rather, it is likely that many of these are amenable to tuning CAR selectivity at little or no cost
362 to the maximal signalling response, provided that the target antigen is overexpressed on malignant cells. Our CAR
363 display platform facilitates this process by enabling library generation and high-throughput functional screening.
364 The simplicity of this method may present notable advantages versus more complex approaches (e.g.,
365 combinatorial logic gates and soluble molecules) that have been put forward to deal with off-tumour toxicity
366 effects. Alternatively, engineering CAR selectivity based on antigen affinity could be combined with such
367 methods. For instance, multi-specific CAR T cells have recently been developed that integrate the recognition of
368 two targets^{49, 50, 51}. In such a system, it is crucial that no single binding domain can trigger a cytotoxic response on
369 its own¹⁶. Such constructs could potentially be balanced by tuning CAR antigen binding as described here.
370 Functional display platforms can thus accelerate the development of increasingly sophisticated cell-based
371 immunotherapy treatments that are both effective and safe.

372

373 METHODS

374 *Cell culture*

375 B3Z cells were cultured in Iscove's Modified Dulbecco's Medium (IMDM) with Glutamax; SKBR3, MCF-7 and
376 HEK293 cells were cultured in Dulbecco's Modified Eagle Medium (DMEM) (Gibco). Culture media were
377 supplemented with 10% fetal bovine serum, 1% Penicillin-Streptomycin (Gibco) and 100 µg/mL Normocin
378 (Invivogen). For passages and experiments, adherent cell lines were detached using TrypLE™ Express (Thermo
379 Fischer) at 37°C.

380

381 *Genome editing and sequencing*

382 Genomic modifications of B3Z cells were performed by CRISPR/Cas9 genome editing. Guide RNA (gRNA) was
383 assembled as a crRNA (Supplementary Table 2) and tracrRNA duplex according to the manufacturer's instructions
384 (IDT). For cell lines without endogenous Cas9 expression, a ribonucleoprotein (RNP) was assembled by
385 incubating the duplex RNA and *Streptococcus pyogenes* Cas9-V3 (IDT) at room temperature for 20 min. For
386 amplimer HDR, a double-stranded DNA repair template was generated by PCR with flanking homology arms of
387 ~700 bp in length; 5 µg of purified product was used for the transfection. For ssODN HDR, 500 pmol ultramer
388 (IDT) was used. Transfections (electroporations) were carried out using a Lonza 4D-Nucleofector according to
389 recommended protocols. Briefly, 500,000 B3Z cells were collected and resuspended in SF buffer. The RNP/DNA
390 mixture was added to the cells in a 1:10 ratio for a total volume of 100 µL. Electroporations were performed in
391 Nucleocuvettes with the program CA-138. Cells were then diluted in 600 µL warm medium. Assays or sorting
392 were performed at least four days later. To confirm genome editing, genomic DNA was extracted from at least 10⁴
393 harvested cells using the QuickExtract protocol (Lucigen). The target locus was then amplified by PCR with
394 forward and reverse primers where at least one primer annealed outside the integration site (Supplementary Table
395 1). Sanger sequencing was used to confirm correct integration of HDR templates.

396

397

398 *Flow cytometry and cell labeling*

399 The expression of surface markers or of the genetically-integrated green fluorescence protein (GFP) were
400 assessed by flow cytometry. Cells were first washed in Dulbecco's PBS (DPBS) prior to labeling. For CAR
401 detection, labeling with 1:200 biotinylated anti-Strep tag antibody (GenScript) was followed by 1:500
402 BrilliantViolet 421 conjugated with Streptavidin (Biolegend). To assess HER2 binding, cells were incubated with
403 2.5 μ g/mL soluble HER2 antigen (Merck) and then with 1:250 APC-labeled anti-human HER2 antibody
404 (Biolegend). The same antibody and concentrations were used to measure surface HER2 expression on cell lines
405 SKBR3, MCF-7 and HEK293. For TCR expression, cells were stained with 1:200 APC-labeled anti-mouse
406 V β 5.1/5.2 antibody (Biolegend). For CD3 ϵ expression, cells were stained with 1:200 APC-labeled anti-mouse
407 CD3 ϵ antibody (Biolegend). Cells were kept in DPBS on ice until analytical flow cytometry or FACS. Flow
408 cytometry data were analysed by Flowjo.

409

410 *Co-culture assays and sorting*

411 CAR-expressing B3Z cells were co-cultured in a 1:1 ratio with HER2-expressing cells (SKBR3, MCF-7 or
412 HEK293) in B3Z medium for 16 hours. All cells were then collected, washed in DPBS and stained for flow
413 cytometry analysis or sorting. For assays, 2.5x10⁴ B3Z cells were used, while 3x10⁶ cells were used for sorting.

414

415 *Deep mutational scanning*

416 The DMS CAR library was generated by CRISPR-Cas9 genome editing of the 4D5 CDRH3 with a pool of single-
417 stranded DNA HDR mutant repair templates, as done previously³¹. Briefly, gRNA targeting the CDRH3 of the
418 anti-HER2 CAR in the CAR T cell platform was used to obtain a monoclonal T cell line with a frameshift deletion
419 abrogating CAR expression. This deletion was then repaired with a pool of HDR templates encoding single amino
420 acid substitutions of the CDRH3. The pool was designed with tiled degenerate codons such that all possible amino
421 acid substitutions were represented along 10 positions of the CDRH3. The HDR templates were transfected in the
422 non-CAR expressing T cells, along with gRNA targeting the CDRH3 deletion. To identify enriched CAR variants
423 post-selection, deep sequencing of the libraries was done by a nested PCR strategy to amplify a 401 bp fragment
424 from genomic DNA, which included the CDRH3. A first PCR was performed to amplify the entire CAR transgene;
425 the product was then used as a template for amplification of the smaller CDRH3-containing region. Second, the
426 product was used in a PCR with primers CDRH3_seq_F and CDRH3_seq_R (Supplementary Table 1). The
427 resulting fragments were purified and sequenced by GENEWIZ (Leipzig, Germany). Only sequences with a
428 complete CDR3 harboring a single amino acid substitution (resulting from DMS) were considered in the analysis.
429 The relative abundance of each variant was extracted and used to calculate enrichment ratios with respect to the
430 initial CAR library ("NNK" in the text).

431

432 *Recombinant expression and measurement of scFv binding to antigen*

433 Soluble scFv proteins were recombinantly expressed: the coding sequences were cloned in a bacterial pET28
434 expression vector with a C-terminal His tag and transformed into BL21-DE3 competent *E. coli* cells (NEB). Cells
435 were grown in LB medium at 37°C to an optical density at 600 nm (OD₆₀₀) of 0.6 and protein expression was
436 induced with 1 nM IPTG for 24 hours at 20°C. Cells were then harvested by centrifugation, and proteins were
437 recovered from the periplasm by sonication. TALON metal affinity chromatography was used for purification as
438 previously described⁵². ELISA assays were done with material and reagents from Thermo Fisher Scientific. For

439 this, soluble HER2 antigen was first biotinylated with the EZ-Link™ NHS-PEG4-Biotin reagent for eventual
440 detection. Nunc Maxisorp 96-well plates were coated with 2 µg/mL mouse IgG2b monoclonal 6x-His tag antibody
441 (HIS.H8) and the subsequent blocking was done with ELISA/ELISPOT diluent. The His-tagged scFv proteins
442 were allowed to bind at a concentration of 2 µg/mL, followed by varying concentrations of biotinylated HER2
443 antigen, for 2 hours each. Detection was done with tetramethylbenzidine (TMB) substrate solution and 1:1000
444 Ultra Streptavidin-HRP. The enzymatic reaction was stopped with 0.16 M sulfuric acid. Readings were done with
445 a Infinite Pro M200 plate reader (Tecan) at 450 nm with subtraction at 570 nm.

446

447 **AUTHOR CONTRIBUTIONS**

448 R.B.D.R and S.T.R. designed the study; R.B.D.R., R.C.R., S.F., D.E. and R.V.-L. performed experiments;
449 R.B.D.R., R.C.R. and S.T.R. discussed results. R.B.D.R., R.C.R. and S.T.R. wrote the manuscript with input and
450 commentaries from all authors.

451

452 **ACKNOWLEDGMENTS**

453 We acknowledge the ETH Zurich D-BSSE Single Cell Unit for excellent support and assistance. This work was
454 supported by a ETH Zurich Post-doctoral Fellowship (to R.B.D.R.), a Personalized Health and Related
455 Technologies Post-doctoral Fellowship (to R.V.-L.) and a NCCR Molecular Systems Engineering (to S.T.R.)

456

457 **COMPETING INTERESTS**

458 There are no competing interests to declare

459

460 **DATA AVAILABILITY**

461 The raw FASTQ files from deep sequencing that support the findings of this study will be deposited (following
462 peer-review and publication) in the Sequence Read Archive (SRA) with the primary accession code(s) <code(s)>
463 (<https://www.ncbi.nlm.nih.gov/sra>). Additional data that support the findings of this study are available from the
464 corresponding author upon reasonable request.

465

466 **REFERENCES**

467

- 468 1. Fesnak AD, June CH, Levine BL. Engineered T cells: the promise and challenges of cancer
469 immunotherapy. *Nat Rev Cancer* **16**, 566-581 (2016).
- 470 2. Maude SL, *et al.* Chimeric Antigen Receptor T Cells for Sustained Remissions in Leukemia. *New Engl J
471 Med* **371**, 1507-1517 (2014).
- 472 3. Schuster SJ, *et al.* Chimeric Antigen Receptor T Cells in Refractory B-Cell Lymphomas. *New Engl J
473 Med* **377**, 2545-2554 (2017).
- 474 4. Turtle CJ, *et al.* CD19 CAR-T cells of defined CD4+:CD8+ composition in adult B cell ALL patients.
475 *The Journal of Clinical Investigation* **126**, 2123-2138 (2016).

476

477

478

479

480 5. Kochenderfer JN, *et al.* Chemotherapy-refractory diffuse large B-cell lymphoma and indolent B-cell
481 malignancies can be effectively treated with autologous T cells expressing an anti-CD19 chimeric
482 antigen receptor. *J Clin Oncol* **33**, 540-549 (2015).

483

484 6. MacKay M, *et al.* The therapeutic landscape for cells engineered with chimeric antigen receptors. *Nat
485 Biotechnol*, (2020).

486

487 7. Lamers CHJ, *et al.* Treatment of Metastatic Renal Cell Carcinoma With CAIX CAR-engineered T cells:
488 Clinical Evaluation and Management of On-target Toxicity. *Mol Ther* **21**, 904-912 (2013).

489

490 8. Morgan RA, Yang JC, Kitano M, Dudley ME, Laurencot CM, Rosenberg SA. Case Report of a Serious
491 Adverse Event Following the Administration of T Cells Transduced With a Chimeric Antigen Receptor
492 Recognizing ERBB2. *Mol Ther* **18**, 843-851 (2010).

493

494 9. Richman SA, *et al.* High-Affinity GD2-Specific CAR T Cells Induce Fatal Encephalitis in a Preclinical
495 Neuroblastoma Model. *Cancer Immunol Res* **6**, 36-46 (2018).

496

497 10. Tran E, *et al.* Immune targeting of fibroblast activation protein triggers recognition of multipotent bone
498 marrow stromal cells and cachexia. *J Exp Med* **210**, 1125-1135 (2013).

499

500 11. Yu DH, Hung MC. Overexpression of ErbB2 in cancer and ErbB2-targeting strategies. *Oncogene* **19**,
501 6115-6121 (2000).

502

503 12. Wilson FR, *et al.* Herceptin (R) (trastuzumab) in HER2-positive early breast cancer: a systematic
504 review and cumulative network meta-analysis. *Syst Rev-London* **7**, (2018).

505

506 13. Herrmann F, *et al.* HER-2/neu-mediated regulation of components of the MHC class I antigen-
507 processing pathway. *Cancer Res* **64**, 215-220 (2004).

508

509 14. Maruyama T, *et al.* Inverse correlation of HER2 with MHC class I expression on oesophageal
510 squamous cell carcinoma. *Brit J Cancer* **103**, 552-559 (2010).

511

512 15. Zhao YB, *et al.* A Herceptin-Based Chimeric Antigen Receptor with Modified Signaling Domains
513 Leads to Enhanced Survival of Transduced T Lymphocytes and Antitumor Activity. *J Immunol* **183**,
514 5563-5574 (2009).

515

516 16. Kloss CC, Condomines M, Cartellieri M, Bachmann M, Sadelain M. Combinatorial antigen recognition
517 with balanced signaling promotes selective tumor eradication by engineered T cells. *Nat Biotechnol* **31**,
518 71-+ (2013).

519

520 17. Fedorov VD, Themeli M, Sadelain M. PD-1-and CTLA-4-Based Inhibitory Chimeric Antigen
521 Receptors (iCARs) Divert Off-Target Immunotherapy Responses. *Sci Transl Med* **5**, (2013).

522

523 18. Lanitis E, *et al.* Chimeric Antigen Receptor T Cells with Dissociated Signaling Domains Exhibit
524 Focused Antitumor Activity with Reduced Potential for Toxicity In Vivo. *Cancer Immunology
525 Research* **1**, 43-53 (2013).

526

527 19. Roybal Kole T, *et al.* Precision Tumor Recognition by T Cells With Combinatorial Antigen-Sensing
528 Circuits. *Cell* **164**, 770-779 (2016).

529

530 20. Cartellieri M, *et al.* Switching CAR T cells on and off: a novel modular platform for retargeting of T
531 cells to AML blasts. *Blood Cancer J* **6**, (2016).

532

533 21. Slaga D, *et al.* Avidity-based binding to HER2 results in selective killing of HER2-overexpressing cells
534 by anti-HER2/CD3. *Sci Transl Med* **10**, (2018).

535

536 22. Gargett T, Brown MP. The inducible caspase-9 suicide gene system as a “safety switch” to limit on-
537 target, off-tumor toxicities of chimeric antigen receptor T cells. *Frontiers in Pharmacology* **5**, (2014).

538

539 23. Schmid DA, *et al.* Evidence for a TCR Affinity Threshold Delimiting Maximal CD8 T Cell Function. *J
540 Immunol* **184**, 4936-4946 (2010).

541

542 24. Caruso HG, *et al.* Tuning Sensitivity of CAR to EGFR Density Limits Recognition of Normal Tissue
543 While Maintaining Potent Antitumor Activity. *Cancer Res* **75**, 3505-3518 (2015).

544

545 25. Drent E, *et al.* A Rational Strategy for Reducing On-Target Off-Tumor Effects of CD38-Chimeric
546 Antigen Receptors by Affinity Optimization. *Mol Ther* **25**, 1946-1958 (2017).

547

548 26. Liu XJ, *et al.* Affinity-Tuned ErbB2 or EGFR Chimeric Antigen Receptor T Cells Exhibit an Increased
549 Therapeutic Index against Tumors in Mice. *Cancer Res* **75**, 3596-3607 (2015).

550

551 27. Song DG, Ye QR, Poussin M, Liu L, Figini M, Powell DJ. A fully human chimeric antigen receptor
552 with potent activity against cancer cells but reduced risk for off-tumor toxicity. *Oncotarget* **6**, 21533-
553 21546 (2015).

554

555 28. Park S, *et al.* Micromolar affinity CAR T cells to ICAM-1 achieves rapid tumor elimination while
556 avoiding systemic toxicity. *Sci Rep-Uk* **7**, (2017).

557

558 29. Arcangeli S, *et al.* Balance of Anti-CD123 Chimeric Antigen Receptor Binding Affinity and Density
559 for the Targeting of Acute Myeloid Leukemia. *Mol Ther* **25**, 1933-1945 (2017).

560

561 30. Karttunen J, Sanderson S, Shastri N. Detection of rare antigen-presenting cells by the lacZ T-cell
562 activation assay suggests an expression cloning strategy for T-cell antigens. *Proc Natl Acad Sci U S A*
563 **89**, 6020-6024 (1992).

564

565 31. Mason DM, *et al.* High-throughput antibody engineering in mammalian cells by CRISPR/Cas9-
566 mediated homology-directed mutagenesis. *Nucleic Acids Res* **46**, 7436-7449 (2018).

567

568 32. Cho JH, Okuma A, Al-Rubaye D, Intisar E, Junghans RP, Wong WW. Engineering Axl specific CAR
569 and SynNotch receptor for cancer therapy. *Sci Rep-Uk* **8**, (2018).

570

571 33. Rydzek J, *et al.* Chimeric Antigen Receptor Library Screening Using a Novel NF-kappa B/NFAT
572 Reporter Cell Platform. *Mol Ther* **27**, 287-299 (2019).

573

574 34. Uchibori R, *et al.* Functional Analysis of an Inducible Promoter Driven by Activation Signals from a
575 Chimeric Antigen Receptor. *Mol Ther-Oncolytics* **12**, 16-25 (2019).

576

577 35. Pogson M, Parola C, Kelton WJ, Heuberger P, Reddy ST. Immunogenomic engineering of a plug-and-
578 (dis)play hybridoma platform. *Nat Commun* **7**, 12535 (2016).

579

580 36. Hawkins RE, Russell SJ, Baier M, Winter G. The Contribution of Contact and Noncontact Residues of
581 Antibody in the Affinity of Binding to Antigen - the Interaction of Mutant D1.3 Antibodies with
582 Lysozyme. *J Mol Biol* **234**, 958-964 (1993).

583

584 37. Hudziak RM, Lewis GD, Winget M, Fendly BM, Shepard HM, Ullrich A. p185HER2 monoclonal
585 antibody has antiproliferative effects in vitro and sensitizes human breast tumor cells to tumor necrosis
586 factor. *Molecular and Cellular Biology* **9**, 1165-1172 (1989).

587

588 38. Lanteri M, Ollier L, Giordanengo V, Lefebvre J-C. Designing a HER2/neupromoter to drive
589 α 1,3galactosyltransferase expression for targeted anti- α Gal antibody-mediated tumor cell killing. *Breast*
590 *Cancer Research* **7**, R487 (2005).

591

592 39. Poul MA, Becerril B, Nielsen UB, Morisson P, Marks JD. Selection of tumor-specific internalizing
593 human antibodies from phage libraries. *J Mol Biol* **301**, 1149-1161 (2000).

594

595 40. Aucher A, Magdeleine E, Joly E, Hudrisier D. Capture of plasma membrane fragments from target cells
596 by trogocytosis requires signaling in T cells but not in B cells. *Blood* **111**, 5621-5628 (2008).

597

598 41. Cho HS, *et al.* Structure of the extracellular region of HER2 alone and in complex with the Herceptin
599 Fab. *Nature* **421**, 756-760 (2003).

600

601 42. Renaud JB, *et al.* Improved Genome Editing Efficiency and Flexibility Using Modified
602 Oligonucleotides with TALEN and CRISPR-Cas9 Nucleases. *Cell Rep* **14**, 2263-2272 (2016).

603

604 43. Chmielewski M, Hombach A, Heuser C, Adams GP, Abken H. T cell activation by antibody-like
605 immunoreceptors: Increase in affinity of the single-chain fragment domain above threshold does not
606 increase T cell activation against antigen-positive target cells but decreases selectivity. *J Immunol* **173**,
607 7647-7653 (2004).

608

609 44. Ghorashian S, *et al.* Enhanced CAR T cell expansion and prolonged persistence in pediatric patients
610 with ALL treated with a low-affinity CD19 CAR. *Nat Med* **25**, 1408-+ (2019).

611

612 45. Valitutti S, Lanzavecchia A. Serial triggering of TCRs: A basis for the sensitivity and specificity of
613 antigen recognition. *Immunol Today* **18**, 299-304 (1997).

614

615 46. Drent E, *et al.* Combined CD28 and 4-1BB Costimulation Potentiates Affinity-tuned Chimeric Antigen
616 Receptor-engineered T Cells. *Clinical Cancer Research* **25**, 4014-4025 (2019).

617

618 47. Zhou Y, Zhao LQ, Marks JD. Selection and characterization of cell binding and internalizing phage
619 antibodies. *Arch Biochem Biophys* **526**, 107-113 (2012).

620

621 48. Jain J, Loh C, Rao A. Transcriptional Regulation of the Il-2 Gene. *Curr Opin Immunol* **7**, 333-342
622 (1995).

623

624 49. Petrov JC, *et al.* Compound CAR T-cells as a double-pronged approach for treating acute myeloid
625 leukemia. *Leukemia* **32**, 1317-1326 (2018).

626

627 50. Wilkie S, *et al.* Dual Targeting of ErbB2 and MUC1 in Breast Cancer Using Chimeric Antigen
628 Receptors Engineered to Provide Complementary Signaling. *J Clin Immunol* **32**, 1059-1070 (2012).

629

630 51. Zhang ER, *et al.* Recombination of a dual-CAR-modified T lymphocyte to accurately eliminate
631 pancreatic malignancy. *J Hematol Oncol* **11**, (2018).

632

633 52. Vazquez-Lombardi R, Nevoltris D, Luthra A, Schofield P, Zimmermann C, Christ D. Transient
634 expression of human antibodies in mammalian cells. *Nat Protoc* **13**, 99-117 (2018).

635

636

637